

Identification of Phosphorylation Sites of TOPORS and a Role for Serine 98 in the Regulation of Ubiquitin but Not SUMO E3 Ligase Activity[†]

Hye-Jin Park, Haiyan Zheng, Diptee Kulkarni, John Kerrigan, Pooja Pungalaya, Ahamed Saleem, and Eric H. Rubin*

Departments of Pharmacology and Medicine, The Cancer Institute of New Jersey, Robert Wood Johnson Medical School, University of Medicine and Dentistry of New Jersey, 195 Little Albany Street, New Brunswick, New Jersey 08901

Received October 10, 2008

ABSTRACT: TOPORS is the first example of a protein that possesses both ubiquitin and SUMO E3 ligase activity. The ubiquitination activity maps to a conserved RING domain in the N-terminal region of the protein, which is not required for sumoylation activity. Similar to other E3 ligases, it is likely that the ubiquitin and sumoylation activities of TOPORS are regulated by post-translational modifications. Therefore, we employed mass spectrometry to identify post-translational modifications of TOPORS. Several putative phosphorylated regions were identified in conserved regions of the protein. We investigated the role of phosphorylation of serine 98, which is adjacent to the RING domain, in both cells and in vitro. Mutation of serine 98 to aspartic acid resulted in an increase in the ubiquitin ligase activity of TOPORS both in cells and in vitro. In addition, this mutation increased the binding of TOPORS to the E2 enzyme UbcH5a both in vitro and in cells. Conversely, a phospho-deficient mutant (S98A) exhibited little change in ubiquitin ligase activity compared to wild-type TOPORS, both in cells and in vitro. Neither of the mutants affected the localization of TOPORS to punctate nuclear regions. In addition, neither mutant affected the SUMO ligase activity of TOPORS in cells or in vitro. Molecular modeling studies support a role for serine 98 in regulating TOPORS–E2 interactions. Our findings indicate that phosphorylation of serine 98 regulates the ubiquitin but not the SUMO ligase activity of TOPORS, consistent with a potential binary switch function for TOPORS in protein ubiquitination versus sumoylation.

TOPORS¹ is a nuclear protein that was originally identified as a topoisomerase I-binding and as a p53-binding protein (p53BP3) (1, 2). Expression and genetic studies implicated TOPORS as a tumor suppressor in colon, lung, and brain malignancies (3–5). TOPORS was shown to function as both a ubiquitin and SUMO E3 ligase for p53 (6, 7). Although TOPORS is the first example of a protein with this dual activity, there are several examples of regulation of protein function by ubiquitination versus sumoylation of the same lysine residue, including Ikbα and PCNA, Tax and NEMO (8–10).

A conserved N-terminal RING domain of TOPORS is necessary for ubiquitin E3 ligase activity (6). By contrast, the RING domain is not required for the SUMO ligase activity of TOPORS, which maps to residues 437 to 574

(11). Post-translational modifications of E3 ligases have been shown to regulate their activity (12–16). In particular, phosphorylation of a ubiquitin or SUMO E3 ligase may influence its activity by affecting E2 enzyme interaction, substrate binding, cellular localization, or protein stability (17, 18). For example, the ubiquitination activity of Cbl is regulated by phosphorylation of a tyrosine residue near the RING domain (19–21). Phosphorylation of this residue was shown to increase the ubiquitin ligase activity of Cbl toward the EGFR receptor and Src Tyr kinase (19, 21), and to affect E2 enzyme binding (19). In addition, the ubiquitination activity of Siah2 (a RING dependent ubiquitin E3 ligase) toward its substrate, PHD, is regulated by phosphorylation of Siah2, which affects its subcellular localization (14).

SUMO E3 ligases are also regulated by phosphorylation. For example, phosphorylation of Ser445 of PIASxα enhances its binding to SUMO-1 (16). DNA damage induces HIPK2 to phosphorylate Pc2, which in turn enhances HIPK2 sumoylation by Pc2 (22).

We questioned whether the E3 ligase activities of TOPORS might be regulated by phosphorylation, and used mass spectrometry to analyze potential phosphorylation sites. We identified serine 98 as a phosphorylated residue that is important in the ubiquitin but not the SUMO E3 ligase activity of TOPORS.

[†] This work was supported by United States Public Health Service Grant CA99951 (E.H.R.) awarded by the National Cancer Institute.

* Address correspondence to this author. E-Mail: eric_rubin@merck.com. Phone: (267) 305-1717. Fax: (267) 305-6402.

¹ Abbreviations: ATP, adenosine 5'-triphosphate; E1, ubiquitin activating enzyme; E2, ubiquitin conjugating enzyme; GFP, Green Fluorescence Protein; GST, glutathione-S-transferase; kDa, kilodaltons (1000 daltons); NB, nuclear body; NP-40, Nonidet P40 (IGEPAL CA-630); PAGE, polyacrylamide gel electrophoresis; PCR, polymerase chain reaction; PEST, proline-, glutamate-, serine- or threonine-rich sequence; PML, promyelocytic leukemia protein; PMSF, phenylmethyl-sulfonyl fluoride; RING, really interesting new gene; RS, arginine-serine or serine-arginine dipeptide repeats; SAE2, SUMO activating enzyme; SUMO-1, small ubiquitin like modifier; Tris-HCl, Tris [hydroxymethyl] aminomethane hydrochloride; TOPORS, topoisomerase I-binding, arginine- and serine-rich protein; Ub, ubiquitin; UbcH5a, ubiquitin conjugating enzyme.

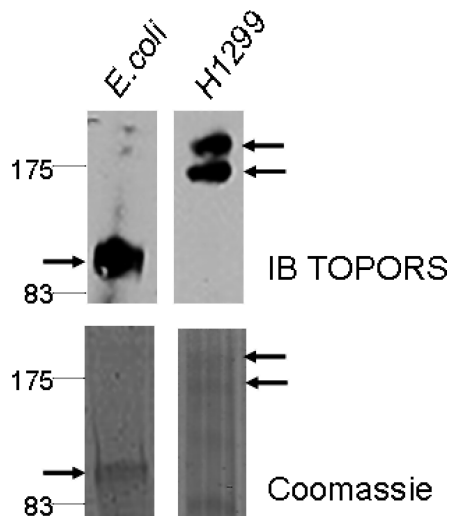


FIGURE 1: Expression and purification of TOPORS from bacteria and H1299 cells. His-tagged TOPORS was overexpressed in bacteria and H1299 cells, then purified by nickel-based affinity chromatography. A representative immunoblot obtained using a TOPORS antibody and a Coomassie blue-stained gel are shown. The arrows indicate bands that were excised for mass spectrometry analyses.

EXPERIMENTAL PROCEDURES

Cell Culture and Transfections. Human cancer cell lines H1299 and HEK293 were grown at 37 °C in DMEM containing 10% FBS and 2% antibiotics in the presence of 5% CO₂. Transfections were performed using Lipofectamine 2000 (Invitrogen, Carlsbad, CA, USA) according to the manufacturer's protocol.

Expression Plasmids. Vectors for mammalian expression of GST-tagged and polyhistidine-tagged TOPORS, as well as for bacterial expression of polyhistidine-tagged TOPORS, were described previously (23). Using these plasmids, site-directed mutagenesis was performed to construct plasmids containing substitutions of alanine or aspartate for serine 98. Briefly, a PCR-based method (Stratagene) was used with the following primers. For alanine: sense, 5'-CCG GCT GATG CAG(<T) CTC CTG ATT CTA AGT GTC C'-3'; antisense, 5'-GGA CAC TTA GAA TCA GGA GC(<A)T GCA TCA GCC GG-3'. For aspartate: sense, 5'-CCA GCT GAT GCA GA(<C)T CCT GAT TCT AAG TGT CC-3'; antisense, 5'-GGA CAC TTA GAA TCA GGA(<G) TCT GCA TCA GCT GG-3'. The resulting plasmids were sequenced to confirm the presence of the expected mutation.

Mass Spectrometric Analyses. His-TOPORS was expressed in H1299 cells or *Escherichia coli* and was purified using nickel-based affinity chromatography. Purified proteins subjected to SDS-PAGE and analyzed by both immunoblotting with a polyclonal TOPORS antibody (6) and by Coomassie blue staining. From the Coomassie gels, 1.5 mm gel slices representing TOPORS bands identified by immunoblotting were in-gel digested with trypsin, Glu C, or AspN, and analyzed by LC-MS/MS as described previously (24). DTA files for MS/MS spectra were generated by Bioworks software (ThermoFinnigan, San Jose, CA) and compiled into mgf (MASCOT generic file) and searched using the MASCOT search engine 2.1 (www.matrixscience.com) against NCBI NR human database with fixed modification of carbamoylmethylation on cysteine and variable modification of phosphorylation (STY) and oxidation of methionine

allowing one missed cleavage. Mass tolerance was set as 2 Da for the parent ion and 0.8 Da for MS/MS. A peptide was considered a significant match if the probability-based MOWSE score was greater than 30. The search results were confirmed manually.

Cellular Ubiquitination and Sumoylation Assays. HEK 293 cells were maintained in Dulbecco's modified Eagle's medium supplemented with 10% fetal bovine serum and antibiotics. Equal numbers of exponentially growing cells were seeded into 6 well plates and transfected using Lipofectamine 2000 (Invitrogen) in the presence of serum- and antibiotic-free media. For ubiquitination assays, cells were cotransfected with 2.5 μ g of pEGFP-TOPORS, pEGFP-TOPORS (S98A) and pEGFP-TOPORS (98D) with or without 500 ng of pMT.107 (expressing His-tagged ubiquitin). For sumoylation assays, cells were cotransfected with 2.5 μ g of pEGFP-TOPORS, pEGFP-TOPORS (S98A) and pEGFP-TOPORS (98D) with or without 500 ng of pcDNA3-His-SUMO-1 (expressing His-tagged SUMO-1). After 24 h transfection, cells were incubated in presence and absence of 4 μ M MG132 for an additional 8 h. Cells were lysed either in SDS sample-loading buffer (60 mM Tris-HCl, pH 6.8, 2% SDS, 10% glycerol, 0.1 M DTT, and 0.1% phenol red) or in 6 M guanidine-HCl. His-tagged SUMO-1 conjugates were purified from guanidine lysates using cobalt-based affinity chromatography as described (6). Lysates were analyzed by immunoblotting with anti ubiquitin (Santacruz), SUMO-1 (Zymed), TOPORS (25), β Actin (cell signaling) antibodies.

Fluorescence Microscopy. HEK 293 cells were grown in glass coverslips and transfected with GFP-Topors wild-type or Topors S98A and S98D mutants. After 24 h transfection, cells were fixed in 3.7% paraformaldehyde in PBS. An Eclipse TE2000 inverted fluorescence microscope equipped with a TE-FM Epi-fluorescence attachment (Nikon) and a SPOT digital camera (Diagnostic Instruments Inc., Sterling Heights, MI) was used to visualize GFP proteins in cells grown in culture dishes. GFP fluorescence was imaged using a GFP filter set (Chroma Technology, Brattleboro, VT) with excitation and emission wavelengths of 450–490 and > 500 nm, respectively.

In Vitro Dual Ubiquitination/Sumoylation Assays. To minimize effects of differential protein concentration on enzymatic assays, we performed ubiquitination and sumoylation reactions in the same tube. Additional experiments were performed using the ubiquitination reagents only. The reactions contained 50 mM HEPES, pH 8.0, 5 mM MgCl₂, 15 μ M ZnCl₂, 4 mM ATP with an ATP-regenerating system (10 mM creatine phosphate (Sigma), 3.5 units/mL creatine kinase (Sigma), and 0.6 units/mL inorganic pyrophosphatase (Sigma)). The reactions contained 3 nM purified GST-TOPORS (wild-type or mutants), 150 nM human UBE1 (Boston Biochem), 150 nM SAE2/SAE1 (Sigma), 300 nM Ubch5a (Boston Biochem), 300 nM Ubch9 (Sigma), 25 μ M ubiquitin (Boston Biochem), and 25 μ M SUMO-1 (Boston Biochem). Reactions were carried out at 30 °C for 30 min in a 30 μ L volume and were terminated by addition of SDS sample buffer (60 mM Tris-HCl, pH 6.8, 2% SDS, 10% glycerol, and 0.1% phenol red) containing 0.1 M DTT. Reaction products were resolved by SDS-PAGE and

Table 1: Phosphorylated and Corresponding Unmodified TOPORS Peptides Detected by LC–MS/MS in H1299 Cells and Bacteria. Using a MASCOT score cutoff of 30, four phosphopeptides of TOPORS were identified in H1299 cells (upper panel)^a

peptide	obsd ^b	M _r		delta ^e
		calc ^c	theor ^d	
⁸⁶⁴ SLpSVEIVYEGK ⁸⁷⁴	652.221	1302.4274	1302.6108	−0.1833
⁴⁹¹ TPELVSpSDEDLGSYEK ⁵⁰⁹	1089.423	2176.8314	2176.93	−0.0985
⁸⁹ LQQTVPADApSPDSK ¹⁰²	768.7625	1535.5104	1535.6868	−0.1764
⁵⁸³ VYpSPYNHR ⁵⁹⁰	558.202	1114.3894	1114.4597	−0.0702
⁸⁶⁴ SLSVEIVYEGK ⁸⁷⁴	612.2595	1222.5044	1222.6444	−0.14
⁴⁹¹ TPELVSSDEDLGSYEK ⁵⁰⁹	1049.419	2096.8234	2096.9637	−0.1402
⁸⁹ LQQTVPADASPDSK ¹⁰²	728.8205	1455.6264	1455.7205	−0.0941
⁵⁸³ VYSPYNHR ⁵⁹⁰	518.1995	1034.3844	1034.4933	−0.1089
*				

^a Using this same cutoff score, both phosphorylated and the corresponding unmodified peptide were detected in H1299 cells, whereas in bacteria (lower panel), only the corresponding unmodified peptides were identified. ^b Observed, measured *m/z* value for the peptide. ^c M_r (calc), peptide mass calculated from observed *m/z* value. ^d M_r (theor), identified TOPORS peptide mass resulting from in silico enzyme digested TOPORS sequence. ^e Delta, the mass difference between the calculated and theoretical peptide masses.

analyzed by immunoblotting using monoclonal antiubiquitin (Santa Cruz Biotechnology) or anti-SUMO-1 (Zymed) antibodies.

In Vitro Binding Assays. For GST pulldown experiments, 50 μg of purified GST or GST-TOPORS (wild-type, S98A or S98D) bound to GSH beads (Amersham Biosciences) were incubated with 40 ng of UbCH5a (Boston Biochem) in 0.3 mL of buffer containing 50 mM HEPES pH 8.0, 0.5% Triton X-100, 150 mM NaCl, 1 mM PMSF, 5 μg/μL leupeptin, 1 μg/μL pepstatin, 5 mM MgCl₂ and 15 μM ZnCl₂ at 4 °C for 30 min. Beads were washed three times with the binding buffer, with the supernatant before the first wash saved for analysis. Bound proteins were eluted with SDS sample buffer, followed by immunoblotting with antibodies recognizing UbCH5a.

Immunoprecipitation. HEK293 cells transfected with GFP and GFP-TOPORS (wild type, S98A and S98D) expression plasmids were lysed in a buffer containing 50 mM Tris-HCl (pH 7.5), 150 mM NaCl, 1% (v/v) Nonidet P-40, 0.1% SDS (v/v), 0.5% sodium deoxycholate, 1 mM PMSF and 1:50-diluted protease inhibitor cocktail (Roche). Cell lysates were clarified by centrifugation and preincubated with 1% BSA (Amresco), normalized mouse serum (Calbiochem) and protein G-agarose beads (upstate) at 4 °C overnight. After centrifugation, GFP antibodies were added to supernatants, followed by incubation at 4 °C for 2 h. Resins were washed four times with lysis buffer and bound proteins were eluted with sodium dodecyl sulfate (SDS) sample buffer (Invitrogen) at 95 °C for 5 min. Proteins were fractionated by 4–20% SDS–polyacrylamide gel electrophoresis (PAGE), onto a nitrocellulose membrane, and UbCH5a was detected with anti-UbCH5a antibody and ECL detection system.

Molecular Modeling. All graphics/workstation-level computations were performed on a Sun Ultra 24 Linux workstation. All molecular dynamics computations were performed on the Ranger supercomputer at the University of Texas at Austin. The human TOPORS sequence (UniProtKB # Q9NS56.1) was used as a starting point for modeling of the RING-finger (Really Interesting New Gene) domain (residues 92 to 154 in the TOPORS sequence). The NMR structure of the viral zinc finger domain (1CHC.PDB) was used as a template for building the homology model of the TOPORS RING domain as the sequence from this structure gave the best alignment with the human TOPORS RING-finger domain for comparative modeling (26). The model was built using the Modeler

(9v4) program (27–29). The crystal structure of the c-Cbl-UbCH7 complex (1FBV.PDB) (17) was used as a guide for manual docking of the TOPORS model to the crystal structure of human UbCH5a (2C4P.PDB) (30). The VMD program was used as a tool for the manual docking work (31).

We used molecular dynamics to relax the structure of the model of the UbCH5a–TOPORS complex. The Amber 10 suite of biomolecular simulation programs was used for all molecular dynamics calculations and results analysis (32). The force field of Duan, et al. was used for all molecular mechanics calculations (33). The cationic dummy atom approach was used to model the zinc ion in the active site of the enzyme (34). The initial models were energy minimized in vacuo to remove bad steric contacts. The model was solvated in a truncated octahedral periodic box of SPC/E water (35) with the overall charge of the system neutralized by the insertion of three sodium ions. A 10 Å short-range cutoff was used for all computations. Long-range electrostatics in the model was treated using the particle mesh Ewald method (36, 37). Each system was subjected to energy minimization of the solvent only followed by minimization of the entire system before dynamics. A 2 fs time step was used for all molecular dynamics work. All bonds to hydrogen were restrained using the “shake” method (38). A preliminary dynamics step restraining motion of the protein while gradually increasing temperature from 0 to 300 K was run for 100 ps. This step was followed by a constant temperature (300 K) and constant pressure (1 bar) production run of 5800 ps (5.8 ns). The protein backbone atoms of the model stabilized after ~3.7 ns of simulation (Figure S1 in the Supporting Information). The graphical illustration was prepared with UCSF Chimera (39).

RESULTS

Identification of Phosphorylation Sites of TOPORS Using Mass Spectrometry. To facilitate identification of post-translationally modified regions of TOPORS, we used mass spectrometry with multiple enzymatic digestions to analyze polyhistidine-tagged TOPORS expressed both in H1299 human lung cancer cells and in bacteria (Figure 1). Both phosphorylated and unmodified peptides were identified, representing 60% coverage of the protein (Table 1, Table S1 in the Supporting Information, and Figure S2 in the

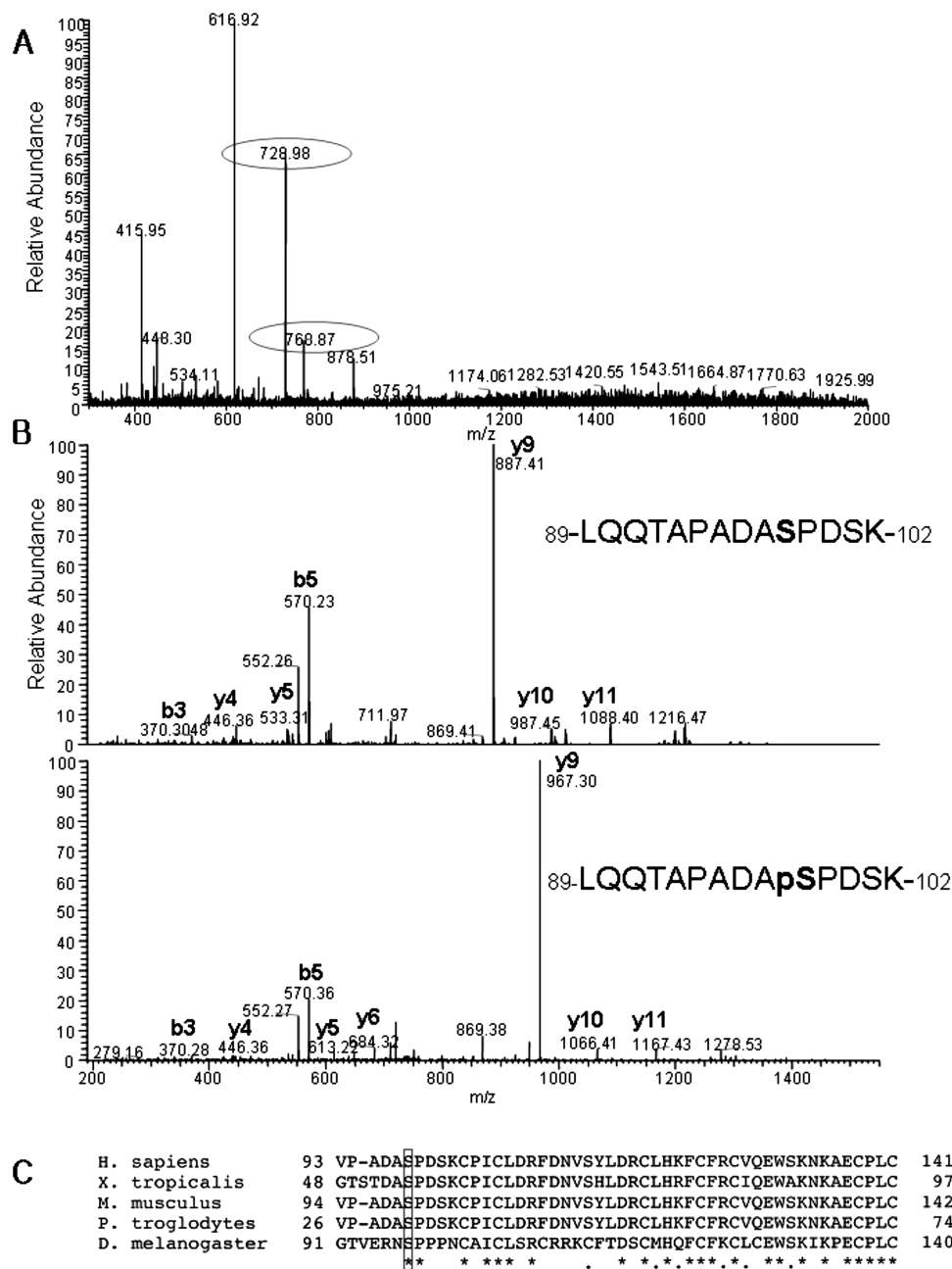


FIGURE 2: Identification of Ser98 as a phosphorylation site in TOPORS by LC-MS/MS. (A) MS spectrum of double-charged parent ions of both a putative phosphopeptide ($^{89}\text{LQQTVPADASPSDK}^{102}$) (m/z 768.86, circled) and the corresponding non-phosphorylated peptide ($^{89}\text{LQQTVPADASPSDK}^{102}$) (m/z 729.21, circled). (B) MS/MS spectrum of m/z 729.21 daughter ion from the non-phosphorylated peptide (upper panel) and that of m/z 768.86 daughter ion from the phosphorylated peptide (lower panel). b and y ion refer to ions containing the N- or C-terminal end of the peptide, respectively. Note pairs of y5 ion peaks from non-phosphorylated and corresponding phosphorylated peptide ions that differ in mass by 80 Da. The presence of y4 and y5 ions localizes the site of phosphorylation to S98. (C) Serine 98 in TOPORS is conserved among species. *Homo sapiens*, *Xenopus tropicalis*, *Mus musculus*, *Pan troglodytes*, *Drosophila melanogaster* TOPORS orthologues were aligned using a ClustalW algorithm. Asterisks indicate identical amino acids. The box indicates the conserved Ser98.

Supporting Information). Importantly, in each case where a phosphorylated peptide was identified in H1299 cells, a corresponding unmodified peptide was identified for TOPORS expressed in bacteria (Table 1). Four putative phosphorylated peptides were identified in mammalian cells, but not in bacteria: Ser98, Ser499, Ser585, and Ser866 (Table 1, Figure 2). Each of these putative phosphosites was confirmed manually. For example, the presence of m/z 446.36 (y4) and 533.31/613.22 (y5/y5 + 80) ion localized the site of phosphorylation in the $^{89}\text{LQQTVPADApSPDSK}^{102}$ peptide to S98 (Figure 2). Peptides with both phosphorylated and non-phosphorylated forms were detected in H1299 cells.

Although we cannot exclude the possibility that dephosphorylation occurred during or after cell lysis, this finding suggests that both phosphorylated and non-phosphorylated forms of TOPORS are present in proliferating H1299 cells (Figure 2). Phosphorylation of Ser98 of TOPORS was reported previously in a screen for nuclear phosphorylated proteins in HeLa cells (40, 41) and this residue is located near the conserved RING domain, which was shown to be required for the ubiquitin ligase activity of TOPORS (6). Therefore, we chose to investigate whether Ser98 might be important in regulating the ubiquitin ligase activity of TOPORS, and

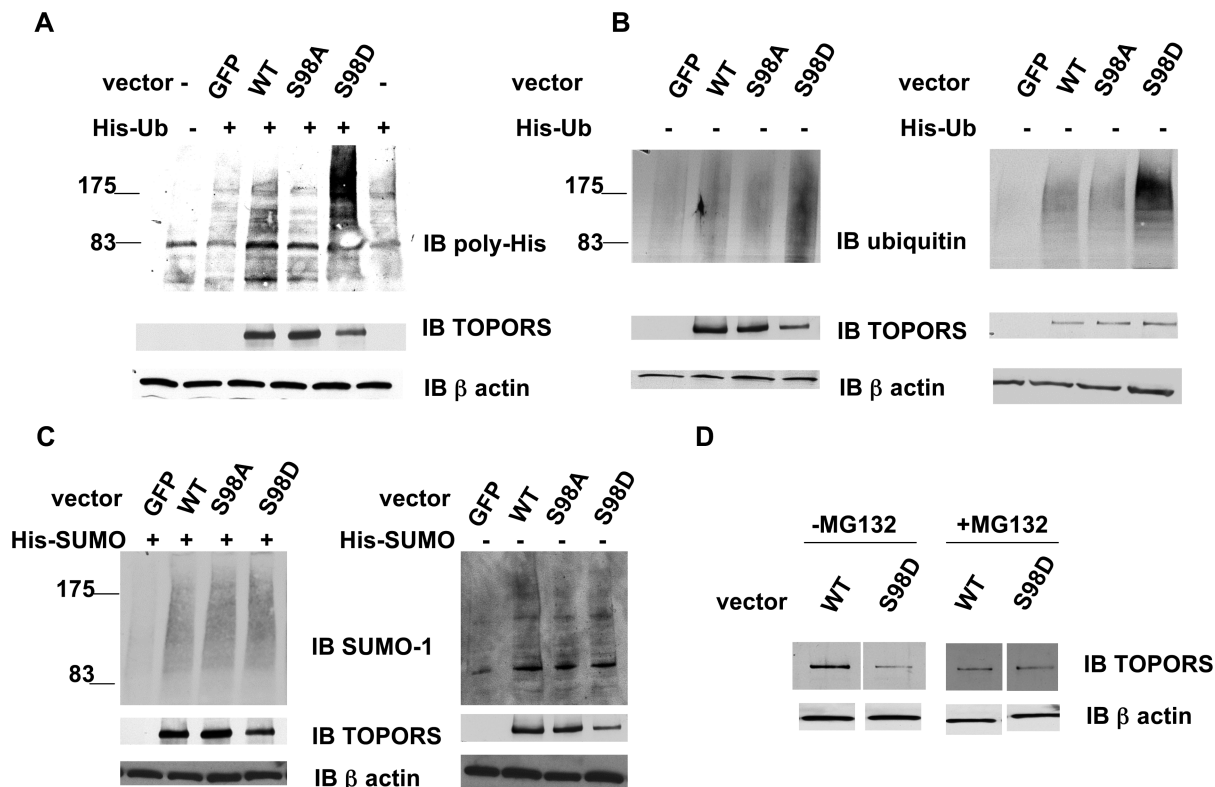


FIGURE 3: Effects of phospho-deficient (S98A) and phosphomimic (S98D) mutants on the ubiquitin and SUMO E3 ligase activities of TOPORS in cells. (A) HEK293 cells were transiently transfected with 500 ng of a plasmid expressing polyhistidine-tagged ubiquitin, along with 2.5 μ g of a plasmid expressing GFP, GFP-TOPORS, or a GFP-TOPORS mutant (S98A or S98D). Cell lysates were analyzed by SDS-PAGE and immunoblotting with antibodies recognizing polyhistidine (top panel), TOPORS (middle panel), or actin (bottom panel). (B) HEK293 cells were transiently transfected with 2.5 μ g of a plasmid expressing GFP, GFP-TOPORS, or a GFP-TOPORS mutant (S98A or S98D). Cell lysates were analyzed as described in A, except that ubiquitin conjugates were analyzed using a ubiquitin antibody. In the right panel the amount of lysate in each lane was adjusted to equal amounts of TOPORS protein. (C) HEK293 cells were transiently transfected with 500 ng of a plasmid expressing polyhistidine-tagged SUMO-1, along with 2.5 μ g of a plasmid expressing GFP, GFP-TOPORS, or a GFP-TOPORS mutant (S98A or S98D). Cell lysates were analyzed by SDS-PAGE and immunoblotting with antibodies recognizing polyhistidine (top panel), TOPORS (middle panel), or actin (bottom panel). The right panel shows the results of transfections of TOPORS plasmids alone. In this case SUMO conjugates were detected using an antibody recognizing SUMO-1. (D) Cells were transfected with expression plasmids for wild-type GFP-TOPORS or the phosphomimic mutant (S98D). After 24 h, cells were left untreated or exposed to 2.5 μ M MG132 for 4 h. Cell lysates were prepared and subjected to immunoblotting using TOPORS and actin antibodies.

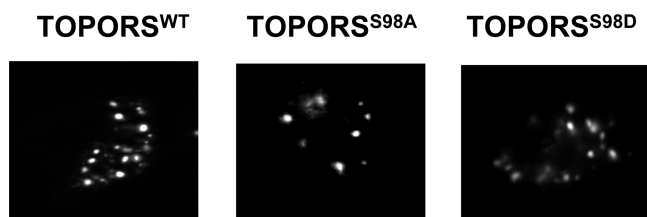


FIGURE 4: Mutation of Ser98 does not affect the cellular localization of TOPORS. HEK393 cells were transfected with plasmids encoding GFP tagged TOPORS (wild type, S98A or S98D mutant) and examined via fluorescent microscopy. Shown are representative images of transfected cells.

constructed and analyzed phospho-deficient (S98A) and phosphomimic (S98D) mutants in cells and *in vitro*.

Analysis of the Effects of Mutations of Serine 98 on the Ubiquitination/Sumoylation Activity of TOPORS in Cells. Since physiologic substrates of TOPORS are not yet known, to investigate the role of phosphorylation of Ser98, we took advantage of the finding that TOPORS is capable of inducing both polymeric ubiquitin (6) and polymeric SUMO-1 chains (42) (Kulkarni, et al., manuscript submitted) in the absence of a specific substrate. In HEK293 cells cotransfected with vectors expressing polyhistidine-tagged ubiquitin and a phosphomimic TOPORS mutant (S98D), there was an

increase in steady-state levels of high molecular weight ubiquitin conjugates, relative to cells expressing wild-type TOPORS (Figure 3A). By contrast, mutation of serine 98 to alanine had no detectable effect on formation of high molecular weight ubiquitin conjugates relative to wild-type TOPORS (Figure 3A). Similar results were obtained in cells transfected with TOPORS vectors alone, in the absence of expression of polyhistidine-tagged ubiquitin (Figure 3B). In both transfection strategies, we noted that expression of the S98D TOPORS mutant was lower than that of the wild-type or S98A mutant (Figure 3B). Similar decreased expression of the S98D mutant was observed in transfections performed using H1299 cells, indicating that this phenomenon is not cell-line specific (Figure 3 in the Supporting Information). When HEK293 cell lysates were equilibrated for relative TOPORS protein expression, an even greater effect of the S98D mutant on high molecular weight ubiquitin conjugates was observed (Figure 3B, right panel). To determine whether the S98D mutation affected protein stability, we transfected cells in the absence or presence of the proteasome inhibitor MG132. Addition of MG132 abrogated the decrease in expression of the phosphomimic mutant (S98D) (Figure 3D). This result suggests that the S98D mutation destabilizes

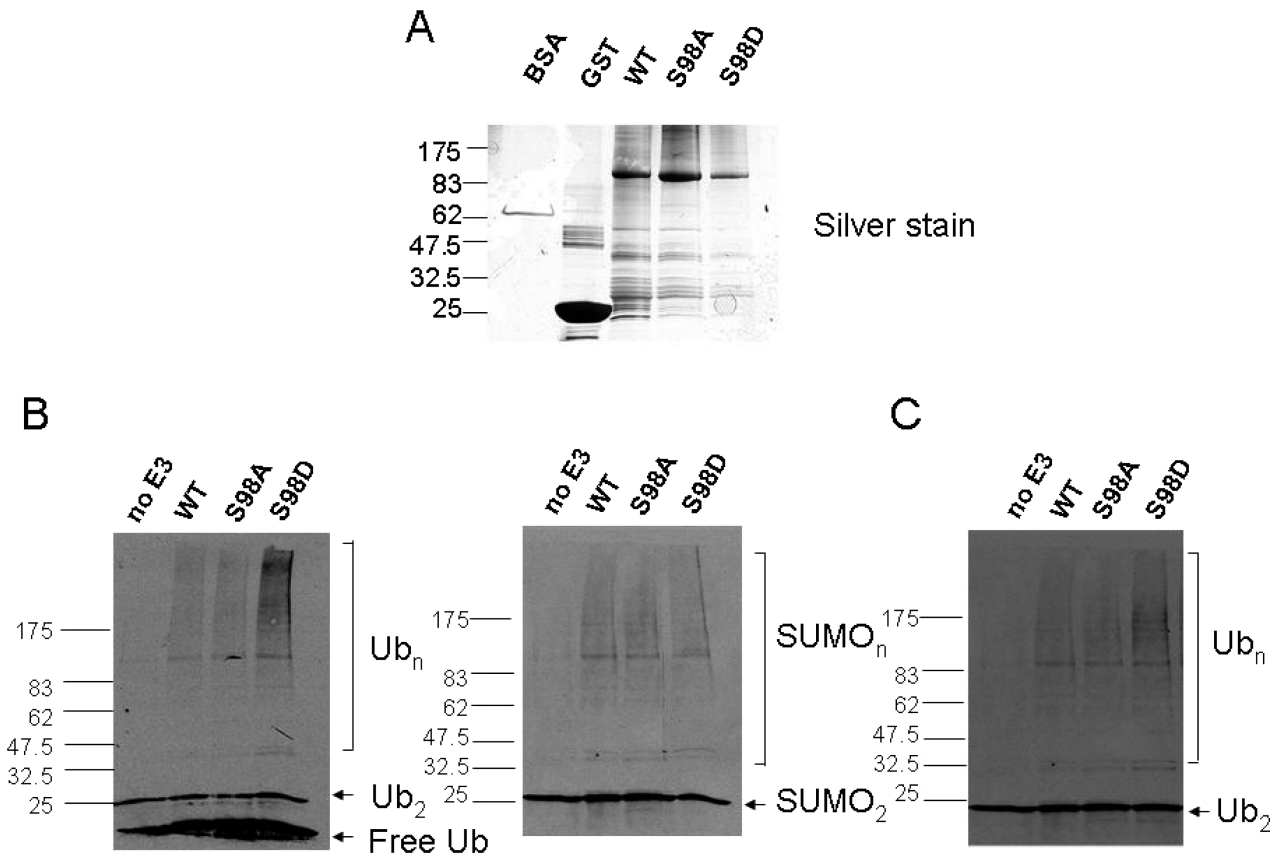


FIGURE 5: Effects of phospho-deficient (S98A) and phosphomimic (S98D) mutants on the ubiquitin and SUMO E3 ligase activities of TOPORS *in vitro*. (A) Silver stain of purified recombinant GST- TOPORS fusion proteins. (B) *In vitro* dual ubiquitin/SUMO ligase reactions were performed using an ATP-regenerating system with either no E3, or wild-type, S98A, or S98D GST-TOPORS proteins. Concentrations of the E1, E2, modifier (ubiquitin or SUMO-1) were 150 nM, 250 nM, and 25 μ M, respectively. Reaction products were divided into two equal portions, and analyzed by immunoblotting with ubiquitin and SUMO-1 antibodies. Brackets indicate the migration of polymeric ubiquitin or SUMO-1 conjugates, with the migration of free ubiquitin, diubiquitin, and di-SUMO-1 indicated by arrows. (C) *In vitro* ubiquitination reactions were performed using the ubiquitination components described in (B), except in the absence of sumoylation components. Reaction products were analyzed using immunoblotting with a ubiquitin antibody. Brackets indicate the migration of polymeric ubiquitin conjugates, with the migration of diubiquitin indicated by an arrow.

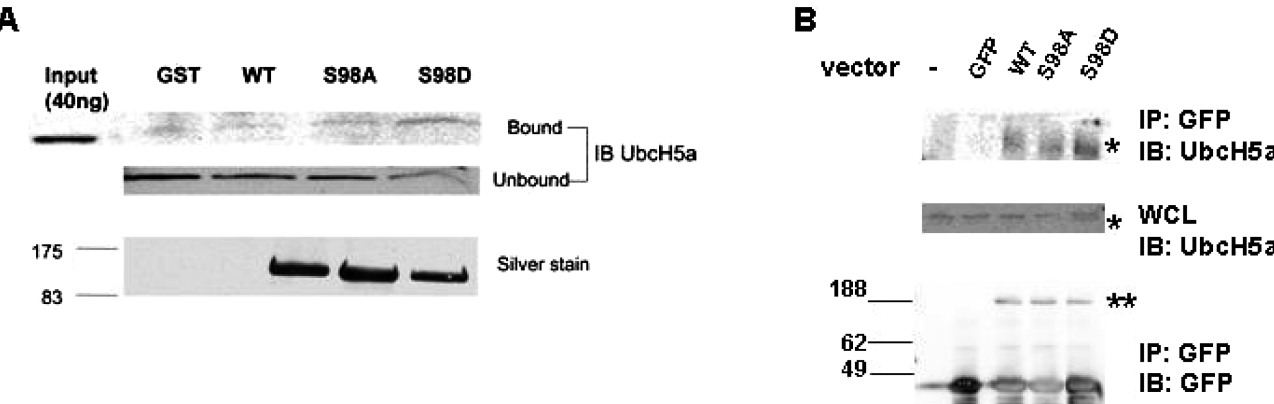


FIGURE 6: Mutation of serine 98 to aspartate increases UbcH5a binding to TOPORS *in vitro* and in cells. (A) Binding of purified UbcH5a (input) to GST or to the indicated GST-TOPORS fusion proteins was assayed as described in Experimental Procedures. Bound proteins and unbound proteins (supernatant before washing beads) were subjected to SDS-PAGE, followed by immunoblotting with UbcH5a antibodies. A silver stain of purified GST-TOPORS (wild-type, S98A and S98D) proteins used in the *in vitro* binding assay is shown in the bottom panel. (B) As indicated, HEK293 cells were transfected with vectors expressing GFP, GFP -TOPORS, or GFP-TOPORS S98A or S98D mutants. After 24 h, the cells were lysed and immunoprecipitated with GFP antibodies as indicated in the Experimental Procedures. Immunoprecipitates were analyzed by antibodies recognizing UbcH5a (top panel) and GFP (bottom panel). Whole cell lysates used for the immunoprecipitations were also analyzed by immunoblotting with a UbcH5a antibody (middle panel). Single asterisks indicate the migration of UbcH5a and double asterisks indicate the migration of GFP-TOPORS proteins.

TOPORS and results in increased proteasome-dependent degradation.

We also tested whether mutation of serine 98 affected TOPORS SUMO ligase activity. In cells cotransfected with vectors expressing polyhistidine-tagged SUMO-1 and TOPORS, there was no difference in the levels of high molecular weight SUMO-1 conjugates among cells expressing wild-type, S98D, or S98A TOPORS proteins (Figure 3C). Similar

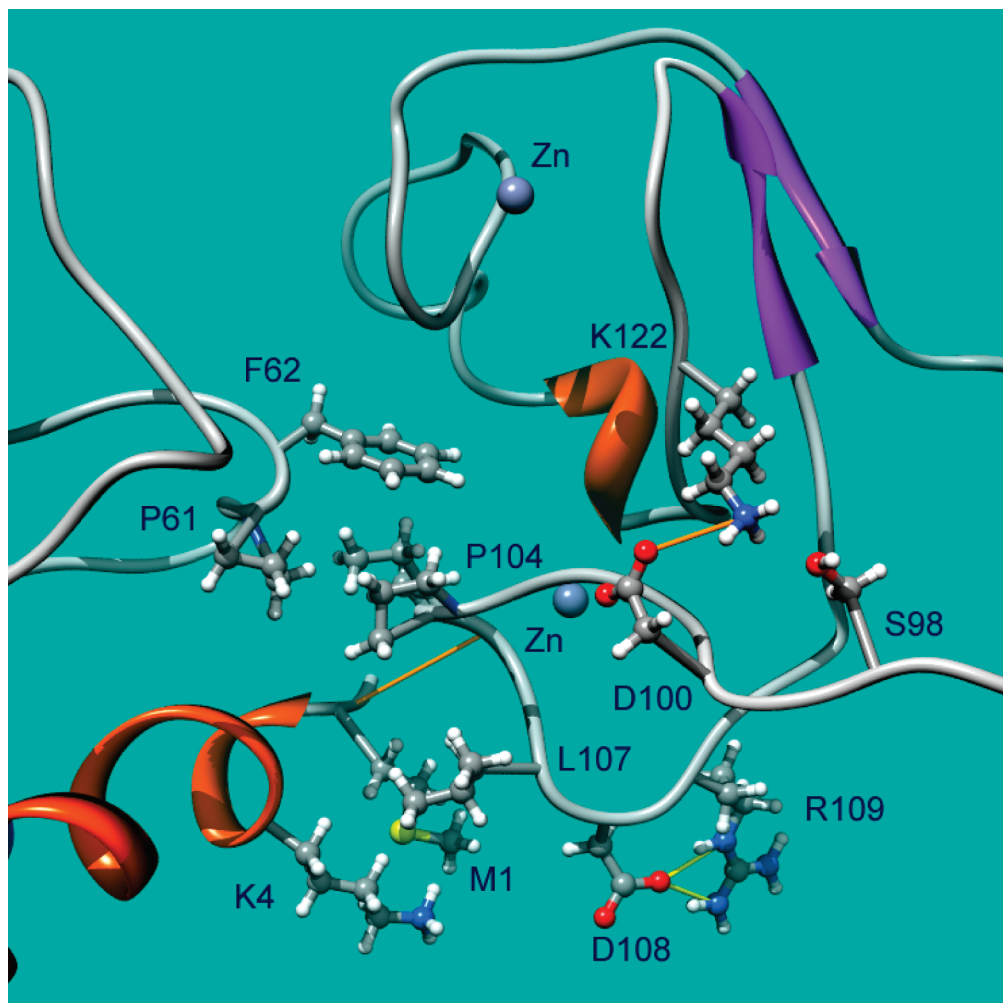


FIGURE 7: Modeling of the interaction between the serine 98 region of TOPORS and UbcH5a. Molecular modeling was performed using the Modeler (9v4) program as indicated in the Experimental Procedures. Graphic illustrating the key residues involved in maintaining backbone conformation in proximity to the conserved S98 residue in the TOPORS RING domain. The two zinc ions are depicted as gray spheres. Hydrogen bonding and salt bridge interactions are indicated by yellow (stronger) and orange (weaker) lines. Note hydrogen bond between backbone atoms of M1 (UbcH5a) and I105 (TOPORS, hidden behind P104).

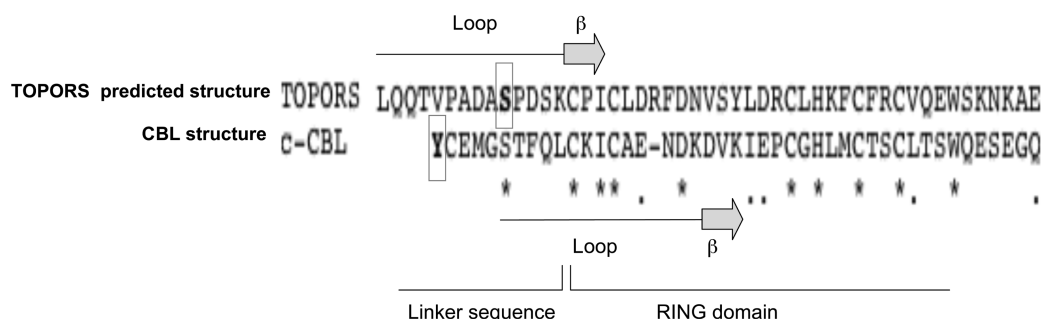


FIGURE 8: Similarity of the phosphorylated residues adjacent to the RING domains of TOPORS and CBL. Phosphorylated Tyr371 of c-Cbl and the putative phosphorylated Ser98 of TOPORS are shown in bold and are boxed. The structure of c-Cbl linker and the RING domain has been described previously (17). Asterisks indicate identical amino acids. Dots indicate amino acids with similar characteristics. The putative structure of TOPORS in this region was determined by a prediction algorithm (www.predictprotein.org).

results were obtained in cells transfected with TOPORS vectors alone, in the absence of expression of polyhistidine-tagged SUMO (Figure 3C). This finding suggests that in contrast to ubiquitination, mutation of serine 98 has no effect on the sumoylation activity of TOPORS.

Since we previously demonstrated that TOPORS colocalizes with PML nuclear bodies in a dynamic manner (25), we investigated whether alteration of S98 affected the cellular localization of TOPORS. Transfection studies with GFP-

TOPORS constructs indicated that neither S98D nor S98A mutations affected the punctate nuclear localization pattern of TOPORS in proliferating cells (Figure 4).

Analysis of the Effects of Mutations of Serine 98 on the Ubiquitination/Sumoylation Activity of TOPORS in Vitro. To directly investigate the role of serine 98 in the ubiquitination and sumoylation activity of TOPORS, we performed in vitro assays using purified components and GST-TOPORS fusions proteins expressed in bacteria. Previous studies indicated that

under these conditions TOPORS was capable of stimulating formation of polymeric ubiquitin (6) and SUMO conjugates (Kulkarni et al., manuscript submitted) in the absence of a specific substrate. This dual activity of TOPORS allowed us to assay the ubiquitination and sumoylation activity of the S98 mutants in a single tube assay. Using this approach and equal amounts of the wild-type and mutant proteins, a greater accumulation of high molecular weight ubiquitin conjugates was observed with the S98D mutant compared to wild-type or the S98A mutant (Figure 5B). Similar results were obtained in when only ubiquitination components were included in the reaction (Figure 5C). Importantly, mutation of serine 98 had no effect on the relative sumoylation activity of TOPORS (Figure 5). Thus, consistent with the cellular transfection data, a phosphomimic mutation of S98 conferred an increase in the ubiquitination but not sumoylation activity of TOPORS *in vitro*.

Mutation of S98 of TOPORS Affects Binding to the E2 Enzyme UbcH5a. RING domains of E3 ubiquitin ligases were shown to bind E2 enzymes, with specific residues both within and adjacent to the RING domain involved in this binding (43, 44). In addition, a structural study of the Cbl–UbcH7 complex suggested that phosphorylation of residue Tyr371 on c-Cbl increased its ubiquitination activity by affecting E2 binding (17, 19, 21). Previously, it was reported that TOPORS stimulated p53 ubiquitination with selected E2 enzymes (UbcH5a, UbcH5c, and UbcH6, but not UbcH7, CDC34, or UbcH2a) (6). We chose UbcH5a to investigate whether S98 of TOPORS was involved in E2 binding, using an *in vitro* pull-down assay with purified GST-TOPORS proteins. We observed minimal binding of UbcH5a to wild-type TOPORS (Figure 6A). Similarly, minimal, if any, UbcH5a binding was detected using the S98A mutant (Figure 6A). By contrast, binding of UbcH5a to the phosphomimic mutant (S98D) was easily detected (Figure 6A). To determine whether the phosphomimic mutant enhanced UbcH5a binding in cells, we performed transient transfection studies using GFP tagged TOPORS expression plasmids (wild type, S98A and S98D). Immunoprecipitation of GFP-tagged TOPORS confirmed that the phosphomimic mutant (S98D) exhibited increased binding to UbcH5a (Figure 6B). This result provides an explanation for the increased ubiquitin ligase activity observed with the S98D mutant in cells and *in vitro*, and suggests that S98 is involved in the binding of UbcH5a to TOPORS.

Molecular Modeling of a TOPORS–UbcH5a Complex. Molecular modeling of a TOPORS–UbcH5a complex was performed to evaluate the impact of S98D mutation or phosphorylation of the S98 side chain on the binding of E2 enzymes by TOPORS (Figure 7). The model indicates that conversion of serine 98 to a negatively charged species (like aspartate or a phosphate conjugate) would lead to charge repulsion with D100 of TOPORS and would compete with D100 for a salt bridge with the side chain of K122 of TOPORS. This could lead to a change in backbone conformation which would impact weaker interactions between K102 and backbone atoms of TOPORS residues L107 and D108. All of these downstream changes in backbone conformation could affect binding of TOPORS to UbcH5a because TOPORS residues 104 to 107 along this stretch of backbone are directly involved in making contacts either to

the E2 UbcH5a (residues M1, K4, P61 and F62) or a zinc ion (Figure 7).

DISCUSSION

In this study, we identified Ser98, Ser499, Ser585, and Ser866 as phosphorylated residues in TOPORS expressed in H1299 cells. Ser98 phosphorylation was reported previously (40, 41). Although we did not investigate other post-translational modifications, sumoylation of TOPORS has also been reported (11). We did not achieve complete coverage of TOPORS, likely due to genesis of short peptides as a result of enzymatic digestion of RS-rich regions.

Similar to proteins involved in RNA splicing (45, 46), it is likely that some or many of the RS dipeptides in TOPORS are phosphorylated in eukaryotic cells. Nevertheless, treatment of His-tagged TOPORS obtained from H1299 cell lysates with calf intestinal alkaline phosphatase (CIP) did not result in a significant decrease in the migration of TOPORS on SDS–polyacrylamide gels (data not shown), suggesting that modifications other than phosphorylation are responsible for the slow gel mobility of TOPORS expressed in mammalian cells compared to bacteria.

While we were particularly interested in S98 due to its proximity to the RING domain, we note that S499, S585, and S866 are all conserved across species, suggesting that they may be important in the regulation of TOPORS. In particular, we note that S499 is located near a SIM-like region (CVIV, residues 478–481). SIM regions are implicated in binding directly to SUMO, and thus it is possible that phosphorylated S499 might regulate the sumoylation activity of TOPORS. Since we used an overexpression (transfection) model to investigate the functional relevance of phosphorylation of serine 98 of TOPORS, the results have to be interpreted with caution. Nevertheless, the results of these transfection studies indicate that phosphorylation of S98 regulates the ubiquitin but not the SUMO ligase activity of TOPORS. Since the N-terminal region of TOPORS (which contains the RING domain) was shown to be dispensable for sumoylation, it is not surprising that mutation of S98 did not affect the sumoylation activity of TOPORS in cells or *in vitro*. It was reported that E3 ubiquitin ligase activities can be enhanced by increased E2 enzyme binding affinity (47, 48). The finding that an S98D phosphomimic mutant of TOPORS increases E2 binding provides an explanation for the increase in ubiquitination activity conferred by this mutant.

The RING domain of TOPORS shares sequence homology with that of the ubiquitin E3 ligase Cbl (17) (Figure 8). Y371 of Cbl was shown to be part of a loop structure that binds the E2 UbcH7 via an α helix, which contacts two loop structures in UbcH7. This interface contains primarily polar and charged residues, which create intermolecular hydrogen bonds (17). The majority of the residues within the Cbl helix, as well as the loop structures of UbcH7, are conserved (49). Tyr phosphorylation of c-Cbl affects its ability to bind to UbcH7 and enhances its ubiquitination activity by changing its conformation (13, 19, 20). Prediction algorithms (www.predictprotein.org) suggest that S98 of TOPORS is also part of a loop (Figure 8). Therefore, it can be speculated that similar to Cbl, S98 of TOPORS is part of a loop structure that is important in E2 binding. The S98 residue is distal in relation to direct binding interactions between TOPORS and

the E2 UbcH5a. Modeling studies of a TOPORS–UbcH5a interaction supports our finding that S98D of TOPORS affects UbcH5a binding. However, it should be emphasized that from the TOPORS–UbcH5a model alone it is not clear whether phosphorylation of S98 would be expected to increase or decrease binding of E2 enzymes by TOPORS. Additional modeling studies of TOPORS with phosphorylated S98 or with an S98D substitution may provide further insight into the role of serine 98 phosphorylation on E2 enzyme binding by TOPORS.

Although we chose UbcH5a to investigate the effect of mutations of S98 on E2–TOPORS interactions, we note that it is not clear whether the UbcH5a–TOPORS interaction is physiologically relevant, and whether additional variables, such as differential expression of E2 enzymes, might be important in regulating E2–TOPORS interactions.

It would be interesting to identify the kinases/phosphatases that regulate the phosphorylation of Ser98 of TOPORS. Predicted kinases for S98 of TOPORS include the CMGC group (cyclin-dependent kinase (CDKs), mitogen-activated protein kinase (MAPKs), glycogen synthase kinase (GSKs), and CDK-like kinase (CLKs)) (50) (<http://pred.ngri.re.kr/PredPhospho.htm>). In addition, Ser98 is part of a SP dipeptide, which is a MAPK consensus site (51). Other predicted kinases for Ser499 include CK2 (www.predict-protein.org).

In summary, we identified Ser98 as a phosphorylated residue in TOPORS that regulates ubiquitination activity, likely by increasing E2 binding affinity. Since mutation of Ser98 does not affect the sumoylation activity of TOPORS, phosphorylation of Ser98 may function as a switch to control ubiquitination versus sumoylation of TOPORS substrates.

ACKNOWLEDGMENT

We thank Jin Woo Jung and Kwang Pyo Kim for assistance with experiments and Peter Lobel for assistance with mass spectrometry.

SUPPORTING INFORMATION AVAILABLE

Table S1 lists TOPORS peptides detected by LC–MS/MS analysis. Figure S1 shows protein sequence coverage by LC–MS/MS analysis using multiple enzymes for digestion, including trypsin, Glu-C and Asp-N. Figure S2 illustrates protein backbone atom rmsd during the course of the molecular modeling stimulation. Figure S3 shows the relative protein expression of TOPORS WT and mutants (S98A and S98D) in H1299 cells, as detected by immunoblotting with a TOPORS antibody. This material is available free of charge via the Internet at <http://pubs.acs.org>.

REFERENCES

- Haluska, P., Jr., Saleem, A., Rasheed, Z., Ahmed, F., Su, E. W., Liu, L. F., and Rubin, E. H. (1999) Interaction between human topoisomerase I and a novel RING finger/arginine-serine protein. *Nucleic Acids Res.* 27, 2538–2544.
- Lin, L., Ozaki, T., Takada, Y., Kageyama, H., Nakamura, Y., Hata, A., Zhang, J. H., Simonds, W. F., Nakagawara, A., and Koseki, H. (2005) topors, a p53 and topoisomerase I-binding RING finger protein, is a coactivator of p53 in growth suppression induced by DNA damage. *Oncogene* 24, 3385–3396.
- Saleem, A., Dutta, J., Malegaonkar, D., Rasheed, F., Rasheed, Z., Rajendra, R., Marshall, H., Luo, M., Li, H., and Rubin, E. H. (2004) The topoisomerase I- and p53-binding protein topors is differentially expressed in normal and malignant human tissues and may function as a tumor suppressor. *Oncogene* 23, 5293–5300.
- Oyanagi, H., Takenaka, K., Ishikawa, S., Kawano, Y., Adachi, Y., Ueda, K., Wada, H., and Tanaka, F. (2004) Expression of LUN gene that encodes a novel RING finger protein is correlated with development and progression of non-small cell lung cancer. *Lung Cancer* 46, 21–28.
- Bredel, M., Bredel, C., Juric, D., Harsh, G. R., Vogel, H., Recht, L. D., and Sikic, B. I. (2005) High-resolution genome-wide mapping of genetic alterations in human glial brain tumors. *Cancer Res.* 65, 4088–4096.
- Rajendra, R., Malegaonkar, D., Pungaliya, P., Marshall, H., Rasheed, Z., Brownell, J., Liu, L. F., Lutzker, S., Saleem, A., and Rubin, E. H. (2004) Topors functions as an E3 ubiquitin ligase with specific E2 enzymes and ubiquitinates p53. *J. Biol. Chem.* 279, 36440–36444.
- Weger, S., Hammer, E., and Heilbronn, R. (2005) Topors acts as a SUMO-1 E3 ligase for p53 in vitro and in vivo. *FEBS Lett.* 579, 5007–5012.
- Johnson, E. S. (2004) Protein modification by SUMO. *Annu. Rev. Biochem.* 73, 355–382.
- Muller, S., Matunis, M. J., and Dejean, A. (1998) Conjugation with the ubiquitin-related modifier SUMO-1 regulates the partitioning of PML within the nucleus. *EMBO J.* 17, 61–70.
- Melchior, F., and Hengst, L. (2002) SUMO-1 and p53. *Cell Cycle* 1, 245–249.
- Weger, S., Hammer, E., and Engstler, M. (2003) The DNA topoisomerase I binding protein topors as a novel cellular target for SUMO-1 modification: characterization of domains necessary for subcellular localization and sumylation. *Exp. Cell Res.* 290, 13–27.
- Swaminathan, G., and Tsygankov, A. Y. (2006) The Cbl family proteins: ring leaders in regulation of cell signaling. *J. Cell. Physiol.* 209, 21–43.
- Kassenbrock, C. K., Hunter, S., Garl, P., Johnson, G. L., and Anderson, S. M. (2002) Inhibition of Src family kinases blocks epidermal growth factor (EGF)-induced activation of Akt, phosphorylation of c-Cbl, and ubiquitination of the EGF receptor. *J. Biol. Chem.* 277, 24967–24975.
- Khurana, A., Nakayama, K., Williams, S., Davis, R. J., Mustelin, T., and Ronai, Z. (2006) Regulation of the ring finger E3 ligase Siah2 by p38 MAPK. *J. Biol. Chem.* 281, 35316–35326.
- He, H., Tan, M., Pamarthy, D., Wang, G., Ahmed, K., and Sun, Y. (2007) CK2 phosphorylation of SAG at Thr10 regulates SAG stability, but not its E3 ligase activity. *Mol. Cell. Biochem.* 295, 179–188.
- Hecker, C. M., Rabiller, M., Haglund, K., Bayer, P., and Dikic, I. (2006) Specification of SUMO1- and SUMO2-interacting motifs. *J. Biol. Chem.* 281, 16117–16127.
- Zheng, N., Wang, P., Jeffrey, P. D., and Pavletich, N. P. (2000) Structure of a c-Cbl-UbcH7 complex: RING domain function in ubiquitin-protein ligases. *Cell* 102, 533–539.
- Winkler, G. S., Albert, T. K., Dominguez, C., Legtenberg, Y. I., Boelens, R., and Timmers, H. T. (2004) An altered-specificity ubiquitin-conjugating enzyme/ubiquitin-protein ligase pair. *J. Mol. Biol.* 337, 157–165.
- Yokouchi, M., Kondo, T., Sanjay, A., Houghton, A., Yoshimura, A., Komiyama, S., Zhang, H., and Baron, R. (2001) Src-catalyzed phosphorylation of c-Cbl leads to the interdependent ubiquitination of both proteins. *J. Biol. Chem.* 276, 35185–35193.
- Kassenbrock, C. K., and Anderson, S. M. (2004) Regulation of ubiquitin protein ligase activity in c-Cbl by phosphorylation-induced conformational change and constitutive activation by tyrosine to glutamate point mutations. *J. Biol. Chem.* 279, 28017–28027.
- Levkowitz, G., Waterman, H., Ettenberg, S. A., Katz, M., Tsygankov, A. Y., Alroy, I., Lavi, S., Iwai, K., Reiss, Y., Ciechanover, A., Lipkowitz, S., and Yarden, Y. (1999) Ubiquitin ligase activity and tyrosine phosphorylation underlie suppression of growth factor signaling by c-Cbl/Sli-1. *Mol. Cell* 4, 1029–1040.
- Roscic, A., Moller, A., Calzado, M. A., Renner, F., Wimmer, V. C., Gresko, E., Ludi, K. S., and Schmitz, M. L. (2006) Phosphorylation-dependent control of Pc2 SUMO E3 ligase activity by its substrate protein HIPK2. *Mol. Cell* 24, 77–89.
- Guan, B., Pungaliya, P., Li, X., Uquillas, C., Mutton, L. N., Rubin, E. H., and Bieberich, C. J. (2008) Ubiquitination by TOPORS Regulates the Prostate Tumor Suppressor NKX3.1. *J. Biol. Chem.* 283, 4834–4840.

24. Jerkic, M., Rodriguez-Barbero, A., Prieto, M., Toporsian, M., Pericacho, M., Rivas-Elena, J. V., Obreo, J., Wang, A., Perez-Barriocanal, F., Arevalo, M., Bernabeu, C., Letarte, M., and Lopez-Novoa, J. M. (2006) Reduced angiogenic responses in adult Endoglin heterozygous mice. *Cardiovasc. Res.* 69, 845–854.
25. Rasheed, Z. A., Saleem, A., Ravee, Y., Pandolfi, P. P., and Rubin, E. H. (2002) The topoisomerase I-binding RING protein, topors, is associated with promyelocytic leukemia nuclear bodies. *Exp. Cell Res.* 277, 152–160.
26. Barlow, P. N., Luisi, B., Milner, A., Elliott, M., and Everett, R. (1994) Structure of the C3HC4 domain by 1H-nuclear magnetic resonance spectroscopy. A new structural class of zinc-finger. *J. Mol. Biol.* 237, 201–211.
27. Marti-Renom, M. A., Madhusudhan, M. S., Fiser, A., Rost, B., and Sali, A. (2002) Reliability of assessment of protein structure prediction methods. *Structure (Cambridge)* 10, 435–440.
28. Marti-Renom, M. A., Stuart, A. C., Fiser, A., Sanchez, R., Melo, F., and Sali, A. (2000) Comparative protein structure modeling of genes and genomes. *Annu. Rev. Biophys. Biomol. Struct.* 29, 291–325.
29. Sali, A., and Blundell, T. L. (1993) Comparative protein modelling by satisfaction of spatial restraints. *J. Mol. Biol.* 234, 779–815.
30. Dodd, R. B., and Read, R. J. (2006) Structures of two human ubiquitin-conjugating enzymes from twinned crystals, unpublished.
31. Humphrey, W., Dalke, A., and Schulten, K. (1996) VMD - Visual Molecular Dynamics. *J. Mol. Graphics Modell.* 14.1, 33–38.
32. Case, D. A., Cheatham III, T. E., Darden, T., Gohlke, H., Luo, H., Merz, K. M., Onufriev, A., Simmerling, C., Wang, B., and Woods, R. (2005) The Amber biomolecular simulation programs. *J. Comput. Chem.* 26, 1668–1688.
33. Duan, Y., Wu, C., Chowdhury, S., Lee, M. C., Xiong, G., Zhang, W., Yang, R., Cieplak, P., Luo, R., Lee, T., Caldwell, J., Wang, J., and Kollman, P. (2003) A point-charge force field for molecular mechanics simulations of proteins based on condensed-phase quantum mechanical calculations. *J. Comput. Chem.* 24, 1999–2012.
34. Pang, Y. P., Xu, K., Yazal, J. E., and Prendergas, F. G. (2000) Successful molecular dynamics simulation of the zinc-bound farnesyltransferase using the cationic dummy atom approach. *Protein Sci.* 9, 1857–1865.
35. Berendsen, H. J., Grigera, J., and Straatsma, T. (1987) The missing term in effective pair potentials. *J. Phys. Chem.* 91, 6269–6271.
36. Darden, T., York, D., and Pedersen, L. (1993) Particle Mesh Ewald: An N-log(N) method for Ewald sums in large systems. *J. Chem. Phys.* 98, 10089–10092.
37. Essmann, U., Perera, L., Berkowitz, M. L., Darden, T., Lee, H., and Pedersen, L. (1995) A smooth particle mesh ewald potential. *J. Chem. Phys.* 103, 8577–8592.
38. Miyamoto, S., and Kollman, P. (1992) SETTLE: An Analytical Version of the SHAKE and RATTLE Algorithms for Rigid Water Models. *J. Comput. Chem.* 13, 952–962.
39. Pettersen, E., Goddard, T., Huang, C., Couch, G., Greenblatt, D., Meng, E., and Ferrin, T. E. (2004) UCSF Chimera - A Visualization System for Exploratory Research and Analysis. *J. Comput. Chem.* 25, 1605–1612.
40. Beausoleil, S. A., Jedrychowski, M., Schwartz, D., Elias, J. E., Villen, J., Li, J., Cohn, M. A., Cantley, L. C., and Gygi, S. P. (2004) Large-scale characterization of HeLa cell nuclear phosphoproteins. *Proc. Natl. Acad. Sci. U.S.A.* 101, 12130–12135.
41. Beausoleil, S. A., Villen, J., Gerber, S. A., Rush, J., and Gygi, S. P. (2006) A probability-based approach for high-throughput protein phosphorylation analysis and site localization. *Nat. Biotechnol.* 24, 1285–1292.
42. Hammer, E., Heilbronn, R., and Weger, S. (2007) The E3 ligase Topors induces the accumulation of polysumoylated forms of DNA topoisomerase I in vitro and in vivo. *FEBS Lett.* 581, 5418–5424.
43. Joazeiro, C. A., and Weissman, A. M. (2000) RING finger proteins: mediators of ubiquitin ligase activity. *Cell* 102, 549–552.
44. Freemont, P. S. (2000) RING for destruction. *Curr. Biol.* 10, R84–87.
45. Ma, C. T., Velazquez-Dones, A., Hagopian, J. C., Ghosh, G., Fu, X. D., and Adams, J. A. (2008) Ordered multi-site phosphorylation of the splicing factor ASF/SF2 by SRPK1. *J. Mol. Biol.* 376, 55–68.
46. Mao, D. Y., Ceccarelli, D. F., and Sicheri, F. (2008) "Unraveling the tail" of how SRPK1 phosphorylates ASF/SF2. *Mol. Cell* 29, 535–537.
47. Joazeiro, C. A., Wing, S. S., Huang, H., Levenson, J. D., Hunter, T., and Liu, Y. C. (1999) The tyrosine kinase negative regulator c-Cbl as a RING-type, E2-dependent ubiquitin-protein ligase. *Science* 286, 309–312.
48. Seol, J. H., Feldman, R. M., Zachariae, W., Shevchenko, A., Correll, C. C., Lyapina, S., Chi, Y., Galova, M., Claypool, J., Sandmeyer, S., Nasmyth, K., Deshaies, R. J., Shevchenko, A., and Deshaies, R. J. (1999) Cdc53/cullin and the essential Hrt1 RING-H2 subunit of SCF define a ubiquitin ligase module that activates the E2 enzyme Cdc34. *Genes Dev.* 13, 1614–1626.
49. Eletr, Z. M., and Kuhlman, B. (2007) Sequence determinants of E2-E6AP binding affinity and specificity. *J. Mol. Biol.* 369, 419–428.
50. Kannan, N., and Neuwald, A. F. (2004) Evolutionary constraints associated with functional specificity of the CMGC protein kinases MAPK, CDK, GSK, SRPK, DYRK, and CK2alpha. *Protein Sci.* 2059–2077.
51. Mylonis, I., Chachami, G., Samiotaki, M., Panayotou, G., Paraskeva, E., Kalousi, A., Georgatsoy, E., Bonanou, S., and Simos, G. (2006) Identification of MAPK phosphorylation sites and their role in the localization and activity of hypoxia-inducible factor-1alpha. *J. Biol. Chem.* 281, 33095–33106.

BI801904Q